Observation of two-dimensional superlattice solitons

M. Heinrich,[1,*] Y. V. Kartashov,[2] L. P. R. Ramirez,[1] A. Szameit,[3] F. Dreisow,[1] R. Keil,[1] S. Nolte,[1] A. Tünnermann,[1] V. A. Vysloukh,[2] and L. Torner[2]

[1]*Institute of Applied Physics, Friedrich-Schiller-University Jena, Max-Wien-Platz 1, 07743 Jena, Germany*
[2]*ICFO–Institut de Ciencies Fotoniques and Universitat Politecnica de Catalunya, Mediterranean Technology Park, Castelldefels, Barcelona 08860, Spain*
[3]*Department of Physics and Solid State Institute, Technion, 32000 Haifa, Israel*
[*]*Corresponding author: heinrich@iap.uni-jena.de*

Received September 8, 2009; revised October 23, 2009; accepted October 24, 2009; posted November 2, 2009 (Doc. ID 116872); published November 24, 2009

We observe experimentally two-dimensional solitons in superlattices comprising alternating deep and shallow waveguides fabricated via the femtosecond-laser direct writing technique. We find that the symmetry of linear diffraction patterns as well as soliton shapes and threshold powers largely differ for excitations centered on deep and shallow sites. Thus, bulk and surface solitons centered on deep waveguides require much lower powers than their counterparts on shallow sites. © 2009 Optical Society of America

OCIS codes: 190.0190, 190.6135.

Since the prediction of discrete solitons in waveguide arrays [1] and their experimental demonstration [2,3] such states were investigated in a number of settings [4–7]. Particular attention has been paid to the precise tuning of soliton properties. Periodic systems with complicated transverse shapes such as photonic superlattices (SLs) open new opportunities for soliton control [8]. Owing to their binary unit cell, such structures provide the possibility to engineer a minigap within the first propagation band [9]. A variety of linear [10–14] and nonlinear phenomena, including formation of gap solitons [9,15], solitons in Bragg gratings [16], and defect gap solitons [17], were demonstrated in SLs. However, experimental investigations of SL solitons were limited to one-dimensional (1D) settings [18,19] so that the features of two-dimensional (2D) entities remain unseen to date. In this Letter, we report the experimental observation of solitons in 2D binary SLs. We show how soliton formation is affected by the choice of the excited sublattice as well as by the presence of surfaces.

To gain insight into the dynamics of soliton formation, we describe the propagation of light with the nonlinear Schrödinger equation for the dimensionless field amplitude q assuming cw illumination,

$$i\frac{\partial q}{\partial \xi} = -\frac{1}{2}\left(\frac{\partial^2 q}{\partial \eta^2} + \frac{\partial^2 q}{\partial \zeta^2}\right) - |q|^2 q - R(\eta,\zeta)q. \qquad (1)$$

Here η,ζ and ξ are the transverse and the longitudinal coordinates normalized to the characteristic transverse scale and diffraction length, respectively. The refractive index profile is given by

$$R(\eta,\zeta) = p_1 \sum_{n,m=-N}^{N} G(nd,md) + p_2 \sum_{n,m=-(N-1)}^{N} G(nd-d/2,md-d/2), \qquad (2)$$

where p_1 and p_2 represent the depths of centered and shifted sublattices, respectively. The separation between sites in each sublattice is designated as d, whereas $G(\eta_k,\zeta_k)=\exp[-(\eta-\eta_k)^2/w_\eta^2-(\zeta-\zeta_k)^2/w_\zeta^2]$ describes the elliptical shape of the individual waveguides with widths (w_η, w_ζ). Among the conserved quantities of Eq. (1) is the total energy flow $U=\int\int_{-\infty}^{\infty}|q|^2 \mathrm{d}\eta \mathrm{d}\zeta$.

In accordance with the experiments we set $N=3$ (i.e., lattices with 85 waveguides), $d=6.4$ (corresponding to a separation of 64 μm between the waveguides in each sublattice), and $w_\eta=1.1$, $w_\zeta=0.3$ (corresponding to individual waveguides with dimensions of 11 μm$\times$3 μm). In the following, the case $p_1>p_2$ is referred to as the D lattice because the central as well as all corner and edge sites belong to the "deeper" sublattice, i.e., the lattice with a higher refractive index. Analogously, the case $p_1<p_2$ is termed the S lattice, with the above mentioned sites then belonging to the "shallower" sublattice. Further we set $p_1=3.00$, $p_2=2.86$ for the D lattice and $p_1=2.86$, $p_2=3.00$ for the S lattice. The value $p_{1,2}=3$ is equivalent to the actual refractive index modulation depth of $\delta n \sim 3.3\times10^{-4}$.

We search for stationary solutions of Eq. (1) residing in the center, on the edge, or in the corner of the form $q=w(\eta,\zeta)\exp(ib\xi)$, where b is the propagation constant, and $w(\eta,\zeta)$ is a real function describing transverse soliton shape. The dependence $U(b)$ for such solutions is nonmonotonic in both S and D lattices. The branches where $\mathrm{d}U/\mathrm{d}b\le 0$ are unstable, whereas $\mathrm{d}U/\mathrm{d}b>0$ corresponds to stable solitons. 2D SL solitons exist above a cutoff propagation constant b_{co} and for powers above the threshold power U_{th}. In contrast to the findings in truncated 1D SLs [19], solitons in 2D D lattices require considerably lower threshold powers for their existence [Fig. 1(a)]. Thus, for the parameters stated above the soliton residing in the central site of the D lattice has a threshold of $U_{th}\approx 0.550$, whereas its S lattice counterpart exists only above $U_{th}\approx 0.929$. This difference is remarkable,

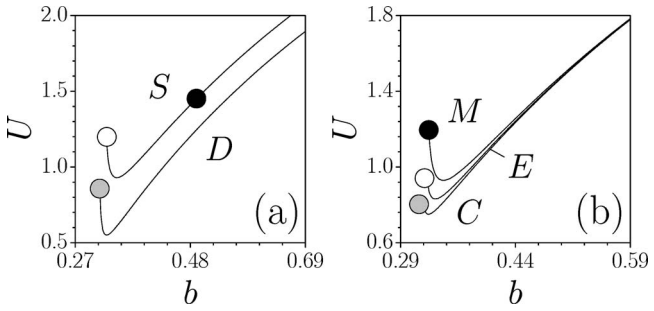

Fig. 1. U versus b for solitons residing in the (a) central sites of D and S lattices and (b) central (M), edge (E), and corner (C) sites of the S lattice. Black, white, and gray circles in (a) correspond to Figs. 2(g), 2(d), and 2(a), while in (b) they correspond to Figs. 2(d)–2(f).

taking into account the small detuning between sublattices of only $|p_2-p_1|/p_2\sim 5\%$. The difference in threshold powers grows rapidly with an increase of $|p_2-p_1|$. In both lattice types corner solitons feature the lowest, and center solitons feature the highest threshold [Fig. 1(b)]. Notice that owing to the finite number of waveguides in the lattice, b_{co} is slightly lower in D lattices.

Representative profiles of 2D SL solitons are shown in Fig. 2. They expand across the lattice and undergo pronounced shape oscillations as $b\rightarrow b_{co}$. However, solitons in the D lattice expand dramatically at b_{co}, covering almost the entire lattice [Figs. 2(a)–2(c)], while their S lattice counterparts extend over only a few neighboring sites when $b\rightarrow b_{co}$ [Figs. 2(d)–2(f)]. This difference in soliton shapes becomes more pronounced with growing detuning $|p_2-p_1|$ between sublattices. Yet, in both S and D lattices an increase in the propagation constant eventually results

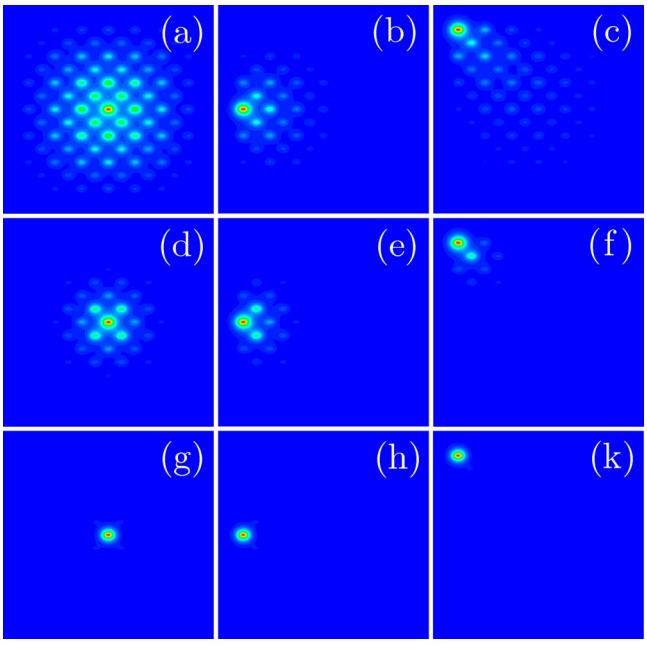

Fig. 2. (Color online) Soliton profiles in the D lattice at (a) $b=0.314$, (b) $b=0.315$, and (c) $b=0.311$. Soliton profiles in the S lattice at (d) $b=0.327$; (e) $b=0.325$; (f) $b=0.322$; and (g),(h),(k) $b=0.491$.

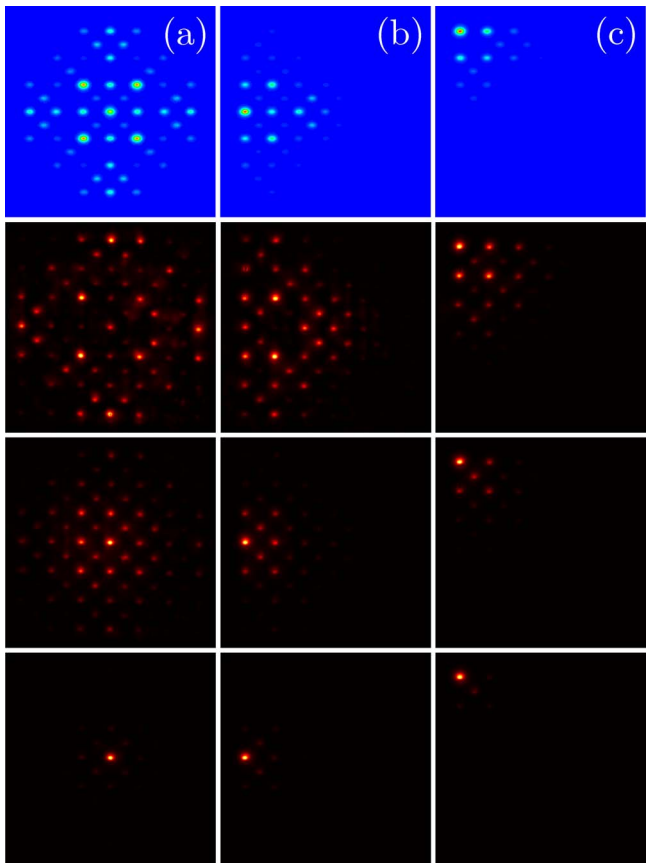

Fig. 3. (Color online) Output patterns for (a) central, (b) edge, and (c) corner excitations in the D lattice. First row, simulated linear patterns. Second row, observed linear pattern at input peak power of 200 kW. Third and fourth rows, observed nonlinear patterns at input peak powers of 1 and 2 MW, respectively.

in the contraction of solitons into the initially excited lattice site as shown for the S lattice in Figs. 2(g), 2(h), and 2(k).

Our experiments were conducted in SLs with the above discussed parameters fabricated via femtosecond-laser direct writing [20] in a fused silica sample with a length of 105 mm. Specific fabrication parameters are discussed in [21]. The waveguides were excited with a Ti:sapphire laser system delivering 200 fs pulses at a wavelength of 800 nm with a repetition rate of 1 kHz. The resulting patterns at the output facet were imaged onto a CCD camera.

Figures 3 and 4 show the output intensity distributions at specific powers for excitations of the central, edge, and corner sites of the D and S lattices, respectively. For comparison, the first rows of both figures show the simulated patterns in the linear regime (vanishing excitation power), while the respective experimental linear patterns (peak power of 200 kW) are depicted in the second row. In the third and fourth rows different stages of localization for peak powers of 1 and 2 MW are shown.

Notice that, while near-threshold stationary solutions generally feature a lower degree of localization in the D lattice, experimental observations suggest that upon dynamical excitation in the nonlinear regime the light spreads more widely in the S lattice at

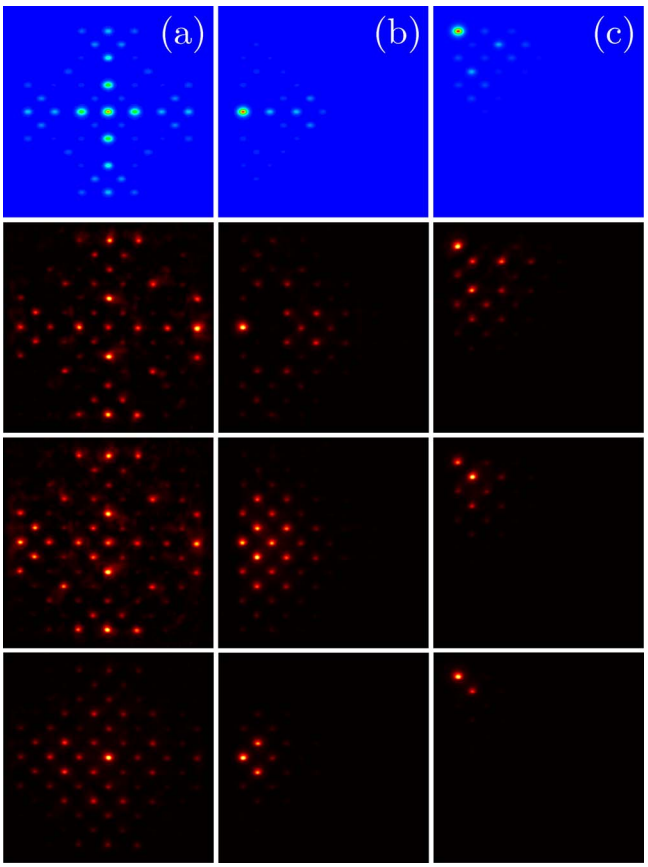

Fig. 4. (Color online) Output patterns for the S lattice. Arrangement corresponds to Fig. 3.

comparable power levels. Figures 3 and 4 illustrate that the experimental localization in D lattices is achieved at substantially lower input peak powers than in S lattices. While in D lattices an increasing input power results in the monotonic contraction of the measured output pattern, an intermediate spreading can be observed in S lattices. This surprising effect occurs when the nonlinear contributions to the effective index of the excited site compensate the detuning between the sublattices, thus leading to a greatly enhanced coupling to the neighboring guides. A similar behavior was observed for the excitation of surface solitons on negative defects [22]. Since all experiments were conducted with pulsed light, the nonlinear index matching may still occur on the pulse slopes, even for peak powers well above the threshold [23]. This results in a more pronounced background and considerably lowers the soliton excitation efficiency in S lattices.

In conclusion, we observed experimentally the formation of solitons residing in the center, edge, and corner sites of binary SLs for both S- and D-type configurations. We showed numerically that even a small refractive index offset between the sublattices has a strong influence on the respective power thresholds. Furthermore, both linear diffraction patterns and soliton profiles may differ substantially depending the excited sublattice.

The authors gratefully acknowledge financial support by the Deutsche Forschungsgemeinschaft (DFS) under Research Unit 532 "Nonlinear spatial-temporal dynamics in dissipative and discrete optical systems," the Leibniz program, and the German Academy of Science Leopoldina (grant LPDS 2009–13).

References

1. D. Christodoulides and R. Joseph, Opt. Lett. **13**, 794 (1988).
2. H. Eisenberg, Y. Silberberg, R. Morandotti, A. Boyd, and J. Aitchison, Phys. Rev. Lett. **81**, 3383 (1998).
3. J. Fleischer, M. Segev, N. Efremidis, and D. Christodoulides, Nature **422**, 147 (2003).
4. F. Lederer, G. I. Stegeman, D. N. Christodoulides, G. Assanto, M. Segev, and Y. Silberberg, Phys. Rep. **463**, 1 (2008).
5. Y. V. Kartashov, V. A. Vysloukh, and L. Torner, Prog. Opt. **52**, 63 (2009).
6. X. Wang, A. Bezryadina, Z. Chen, K. G. Makris, D. N. Christodoulides, and G. I. Stegeman, Phys. Rev. Lett. **98**, 123903 (2007).
7. A. Szameit, Y. V. Kartashov, F. Dreisow, T. Pertsch, S. Nolte, A. Tünnermann, and L. Torner, Phys. Rev. Lett. **98**, 173903 (2007).
8. Y. S. Kivshar and N. Flytzanis, Phys. Rev. A **46**, 7972 (1992).
9. A. A. Sukhorukov and Y. S. Kivshar, Opt. Lett. **27**, 2112 (2002).
10. H. Ohno, E. E. Mendez, J. A. Brum, J. M. Hong, F. Agulló-Rueda, L. L. Chang, and L. Esaki, Phys. Rev. Lett. **64**, 2555 (1990).
11. J. Klos, Phys. Status Solidi B **242**, 1399 (2005).
12. M. Ghulinyan, C. J. Oton, Z. Gaburro, L. Pavesi, C. Toninelli, and D. S. Wiersma, Phys. Rev. Lett. **94**, 127401 (2005).
13. N. Malkova, I. Hromada, X. Wang, G. Bryant, and Z. Chen, Opt. Lett. **34**, 1633 (2009).
14. F. Dreisow, A. Szameit, M. Heinrich, T. Pertsch, S. Nolte, A. Tünnermann, and S. Longhi, Phys. Rev. Lett. **102**, 076802 (2009).
15. Y. J. He, W. H. Chen, H. Z. Wang, and B. A. Malomed, Opt. Lett. **32**, 1390 (2007).
16. K. Yagasaki, I. M. Merhasin, B. A. Malomed, T. Wagenknecht, and A. R. Champneys, EPL **74**, 1006 (2006).
17. W.-H. Chen, Y.-J. He, and H.-Z. Wang, J. Opt. Soc. Am. B **24**, 2584 (2007).
18. R. Morandotti, D. Mandelik, Y. Silberberg, J. S. Aitchison, M. Sorel, D. N. Christodoulides, A. A. Sukhorukov, and Y. S. Kivshar, Opt. Lett. **29**, 2890 (2004).
19. M. I. Molina, I. L. Garanovich, A. A. Sukhorukov, and Y. S. Kivshar, Opt. Lett. **31**, 2332 (2006).
20. K. Itoh, W. Watanabe, S. Nolte, and C. B. Schaffer, MRS Bull. **31**, 620 (2006).
21. A. Szameit, Y. V. Kartashov, V. A. Vysloukh, M. Heinrich, F. Dreisow, T. Pertsch, S. Nolte, A. Tünnermann, F. Lederer, and L. Torner, Opt. Lett. **33**, 1542 (2008).
22. A. Szameit, Y. V. Kartashov, M. Heinrich, F. Dreisow, T. Pertsch, S. Nolte, A. Tünnermann, F. Lederer, V. A. Vysloukh, and L. Torner, Opt. Lett. **34**, 797 (2009).
23. M. Heinrich, A. Szameit, F. Dreisow, R. Keil, S. Minardi, T. Pertsch, S. Nolte, and A. Tünnermann, Phys. Rev. Lett. **103**, 113903 (2009).